



ELSEVIER

Journal of Chromatography A, 877 (2000) 13–24

JOURNAL OF  
CHROMATOGRAPHY A

www.elsevier.com/locate/chroma

## Protein retention in ion-exchange chromatography: effect of net charge and charge distribution

Elisabeth Hallgren<sup>a,1</sup>, Franka Kálmán<sup>b,2</sup>, Dell Farnan<sup>b,3</sup>, Csaba Horváth<sup>b</sup>,  
Jan Ståhlberg<sup>a,\*4</sup>

<sup>a</sup>Department of Analytical Chemistry, Stockholm University, S-10691 Stockholm, Sweden

<sup>b</sup>Department of Chemical Engineering, Yale University, New Haven, CT 06520, USA

Received 2 August 1999; received in revised form 27 January 2000; accepted 8 February 2000

### Abstract

The charge regulated slab model is used to evaluate the salt dependence of the retention of Staphylococcal nuclease A and its mutants in cation-exchange chromatography. An important feature of this work is that the net charge of the proteins is varied in two different ways: (a) by changing the eluent pH so that the charges are created by protonation and (b) by point mutation at position 116. Since the structure of Staphylococcal nuclease and the mutants are known, the pH dependence of retention data of the different mutants gives detailed insights into the retention mechanism. Experimental results show that the salt dependence of retention is affected more strongly by changes of the eluent pH than by point mutations. This implies that the amino acid in position 116 has only a moderately strong interaction with the stationary phase surface and that a patch on one side of the protein surface is mainly responsible for the electrostatic interaction with the surface. © 2000 Elsevier Science B.V. All rights reserved.

**Keywords:** Net charge; Charge distribution; Protein retention; Retention models; Nuclease; Enzymes; Staphylococcal nuclease

### 1. Introduction

Ion-exchange chromatography is a widely used technique for both analytical and preparative separa-

tion of proteins. An advantage of this technique is that the elution takes place under mild conditions so that the protein can maintain its native conformation during the chromatographic process. Protein retention in ion-exchange chromatography is mainly determined by the electrostatic interaction between the solute and the oppositely charged stationary phase surface. By varying the electrolyte concentration in the eluent, the strength of the electrostatic interaction changes so that an increase in the eluent salt concentration attenuates the attraction between the protein and the surface. It is still uncertain which model best describes the ionic strength dependence of this interaction.

\*Corresponding author. Tel.: +46-8-553-27337; fax: +46-8-553-28600.

E-mail address: jan.stahlberg@astrazeneca.com (J. Ståhlberg)

<sup>1</sup>Present address: Amersham Pharmacia Biotech, S-75184 Uppsala, Sweden.

<sup>2</sup>Present address: Solvias AG, CH-4002 Basel, Switzerland.

<sup>3</sup>Present address: Gen-probe Inc., San Diego, CA 92121-1589, USA.

<sup>4</sup>Present address: AstraZeneca Tablet Production Sweden, S-151 85 Södertälje, Sweden.

The first model for ion-exchange chromatography of proteins [1] was introduced by Boardman and Partridge [2] and is based on a stoichiometric ion-exchange process. This ion-exchange process can be written as [3]:



where P is the protein in the mobile phase, C is the counter-ion to the protein, assumed to be monovalent, and S represents the co-ions bound to the stationary phase.  $N_s$  and  $N_c$  are the numbers of salt ions involved in the exchange process. Overbars indicate that the species are adsorbed to the stationary phase.

It is known, however, that due to the long-range nature of the electrostatic interaction, a stoichiometric model cannot give a physically meaningful description of the influence of the eluent ionic composition on protein retention. During the last decade, several non-stoichiometric models for describing protein retention as a function of the salt concentration in the eluent have therefore been proposed. Two of the models [4,5] are based on Manning's ion condensation theory, originally formulated to estimate the properties of cylindrical polyelectrolytes, e.g. DNA molecules, in a salt solution. Another approach has been taken by Noinville et al. [6], who used molecular data on the protein and stationary phase surfaces to calculate the interaction energy by pair-wise summing the electrostatic and dispersive interaction energy for a number of orientations.

The approach most commonly used in colloid and surface chemistry to treat the electrostatic interaction is by solving the Poisson–Boltzmann (P–B) equation. This partial differential equation is obtained from the Poisson equation of classical electrostatics in combination with the Boltzmann distribution [7]. In order to solve the P–B equation, the geometry and the boundary conditions of the system must be specified. It has been possible to find analytical solutions to the P–B equation for one geometry only, the interaction between a charged planar surface and the electrolyte ions in a solution, which constitutes the well-known Gouy–Chapman theory [8,9]. When the electrostatic interaction energy between the charged species in the solution is small compared to their thermal energy, it is possible to approximate the

P–B equation with the linearized P–B equation. This differential equation is much easier to solve and has been solved for several geometries. Roth and Lenhoff [10,11] solved the linearized P–B equation numerically for a sphere interacting with an oppositely charged surface and compared the result with the experimental ionic strength dependence of the adsorption of lysozyme and chymotrypsinogen A to a charged quartz surface. In another paper by Roth et al. [12], the linear superposition approximation was applied to solutions of the linearized P–B equation for a sphere and a planar surface, respectively, to describe electrostatic interactions between a chromatographic surface and an oppositely charged protein.

In the slab model [13], the solution of the linearized P–B equation for two oppositely charged planar surfaces is used as a model for describing the salt dependence of protein retention. The model predicts that the logarithm of the retention factor varies linearly with the reciprocal square root of the ionic strength of the eluent. A large set of experimental data from the literature follows this linear relationship. Cai et al. [14] compared both the slab model and the stoichiometric model of Kopaciewicz et al. [15] with experimental data from combined size exclusion and ion-exchange chromatography of several proteins. They found that the slab model well described the salt dependence of the retention of proteins and also that the charge density of the stationary phase calculated from the model agreed well with the value obtained from titrimetric experiments. The slab model was later expanded to include van der Waals interaction [16] between the surfaces. A recent modification [17] of the slab model includes the charges that are induced at the protein surface by the electrostatic field of the chromatographic surface, the charge regulated slab model.

The slab model allows calculation of the protein net charge from the salt dependence of its retention factor. In these calculations it is assumed that the area of interaction between the protein and the chromatographic surface is equal to half of the total protein area and that the charges are evenly distributed on the protein surface. It is found that the protein net charge calculated by using the model in combination with retention data in most cases compares well with the corresponding protein net charge obtained from titrimetric experiments [13,17]. However, in

some cases discrepancies occur and it is the purpose of this work to investigate the effect of uneven charge distribution at the surface of the protein on its retention behaviour in ion-exchange chromatography.

In this work, the retention in cation-exchange chromatography of a set of mutants from the protein Staphylococcal nuclease type A (*S. nuclease A*) is examined as a function of eluent ionic strength and pH. It has previously been shown that changes in protein net charge due to single point mutations have a significant impact on the ionic strength dependence of protein retention [18]. The essential feature of this study is that the net charge of the protein is varied in two different ways: either by changing the eluent pH or by point mutation. At a given eluent pH, a certain mutant has the same net charge as another mutant has at another pH. Since their net charge is the same, the main difference between such a pair of mutants is that they have a different distribution of ionogenic functions on the protein surface. Differences in the retention behaviour of a set of mutants are used to elucidate the role of an uneven charge distribution on the protein surface in the chromatographic retention.

## 2. Theory

Chromatographic theory shows that the logarithm of the retention factor,  $k'$ , is proportional to the free energy of retention,  $\Delta G_{\text{RET}}$ , of the solute so that:

$$\ln k' = \Delta G_{\text{RET}}/RT + \ln \Phi \quad (2)$$

where  $\Phi$  is the column phase ratio. In this work the free energy of retention is evaluated according to the charge regulated slab model, i.e. from the solution of the linearized P–B equation for two planar oppositely charged surfaces in contact with an electrolyte solution with the possibility of charge regulation. When the charge density of the ion-exchange column is higher than that of the protein,  $\sigma_p$ , the free energy of retention according to this model [17] is given by:

$$\Delta G_{\text{RET}}/A_p = -\sigma_p^2/\kappa\epsilon_0\epsilon_r(1 - K_p) \quad (3)$$

where the inverse Debye length,  $\kappa$ , is related to the ionic strength of the electrolyte,  $I$ , as:

$$\kappa = F(2I)^{1/2}/(\epsilon_0\epsilon_rRT)^{1/2} \quad (4)$$

where  $F$  is Faradays number. In Eq. (3),  $A_p$  is the interacting surface area per mole protein,  $\epsilon_0$  is the permittivity of vacuum,  $\epsilon_r$  is the relative permittivity of the eluent and  $K_p$  is the charge regulation constant. The constant  $K_p$  represents the change in surface charge density of the protein induced by the charges of the oppositely charged stationary phase and has been shown [17] to be equal to:

$$K_p = -\frac{2F^2}{\kappa\epsilon_0\epsilon_r \cdot A_p^0 \cdot RT \ln 10} \cdot \left[ \frac{\partial Z}{\partial \text{pH}} \right] \quad (5)$$

where  $\partial Z/\partial \text{pH}$  is the slope of the pH titration curve of the protein at the pH value of the eluent. Comparison of Eqs. (4) and (5) shows that the  $K_p$  value varies with the eluent ionic strength. In this work a single  $K_p$  value is calculated from the average ionic strength of the eluents in the data set.

Combination of Eqs. (2) and (3) gives the expression for the retention factor according to the charge regulated slab model:

$$\ln k' = \frac{A_p \sigma_p^2}{F(2RT\epsilon_0\epsilon_r)^{1/2}(1 - K_p)} \frac{1}{\sqrt{I}} + \ln \Phi \quad (6)$$

In the calculation it is assumed that the interacting area,  $A_p$ , is equal to one half of the total area of the protein in  $\text{m}^2$  per mole. In Eq. (6), the phase ratio,  $\Phi = A_s^*b/V_0$ , contains the area of chromatographic surface per unit column volume,  $A_s^*/V_0$ , and the adsorption layer thickness,  $b$  [13]. Although the charge regulated slab model shows that  $b$  varies slightly with the ionic strength of the eluent, the variation in the ionic strength interval 50–500 mM is small compared to the first term in Eq. (6).

According to Eq. (6) the slab model predicts a linear relationship between  $\ln k'$  and  $1/\sqrt{I}$ . Indeed, a large set of isocratic retention data for many proteins and stationary phases has been found to exhibit very good linearity [13,17]. Eq. (6) shows that the slope,  $S$ , of the  $\ln k'$  vs.  $1/\sqrt{I}$  plot depends on the square of the charge density on the protein surface. Thus, in combination with the knowledge of the protein surface area, the protein net charge,  $q_{\text{chr}}$ , can be evaluated [17] from the expression:

$$q_{\text{chr}} = \sqrt{\frac{S \cdot (1 - K_p) \cdot A_p^0}{135}} \quad (7)$$

where  $A_p^0$  is the protein surface area in square Ångströms,  $S$  is the slope of the  $\ln k'$  vs.  $1/\sqrt{I}$  plot and 135 is the numerical value of the combined total of the physical constants.

### 3. Experimental

#### 3.1. Instruments

All chromatographic experiments were performed on a Hewlett-Packard (Palo Alto, CA, USA) Model 1090 liquid chromatograph equipped with a DRV5 high-performance pumping system and an auto injector with a 25  $\mu\text{l}$  sampling syringe. A Perkin-Elmer (Norwalk, CT, USA) Model LC-95 variable wavelength UV–Vis detector, fitted with a 1.4  $\mu\text{l}$  flow cell, was used to monitor the absorbance of the column effluent at 280 nm. Data were collected using a DOS mounted version of the Hewlett-Packard Chemstation software, version 1.1. A Hewlett-Packard Vectra 486DX33 computer was used as a platform for this purpose. The detector was connected to the computer through a HP Model 35900 D/A interface. Numerical data were compiled and further analysed using Microsoft Excel. A Model PHM82 pH meter with a No. GK 473901 glass electrode (Radiometer America, Westlake, OH, USA) was used to measure the pH of the buffer solutions. The electrode was calibrated at 25°C and pH 7.00 and 10.00 immediately before use. A 50 $\times$ 4.6 mm column, packed with 10 micron POROS™ S/H bidisperse, giga-porous, strong cation-exchanger particles (Perseptive Biosystems, Framingham, MA, USA), was used. The column bed volume was 0.8 ml, the protein loading capacity of the column was ca. 30 mg/ml and the column dead volume was estimated to be 0.58 ml; i.e. 70% of the column bed volume. The column was thermostated at 25°C.

#### 3.2. Proteins

The variants of nuclease A from *Staphylococcus aureus* were obtained by oligonucleotide directed mutagenesis [19] and the proteins were expressed in

*E. coli*. Physicochemical properties of the variants, including characteristic charge and their hydrodynamic radii at different pH values, have been described in previous publications [20,21].

#### 3.3. Chemicals

Reagent grade sodium chloride, boric acid and sodium borate ( $\text{Na}_2\text{B}_4\text{O}_7 \cdot 10\text{H}_2\text{O}$ ) were supplied by Baxter (Phillipsburg, NJ, USA). Sodium hydroxide pellets were obtained from Mallinckroft (Paris, KY, USA). Deionized water was prepared using a Barnstead (Boston, MA, USA) Nanopure water filtration system. Standard buffer solutions were obtained for the calibration of the pH electrode at pH 10.00 from Brand-Nu Laboratories (Meriden, CT, USA) and at pH 7.00 from J.T. Baker (Phillipsburg, NJ, USA).

#### 3.4. Procedures

Buffered solutions of the eluents were prepared in standard glassware by dissolving the appropriate amount of boric acid and sodium chloride to give the required concentration. The pH of the solution was adjusted with concentrated sodium hydroxide using a glass electrode. In the chromatographic experiments the eluents were pre-mixed and pumped through a single metering pump at a flow-rate of 1 ml/min. Constancy and accuracy of the flow-rate was verified by volumetric methods. Sample solution (20  $\mu\text{l}$ ), containing 1 mg of protein per ml of eluent, was injected at least three times at any given chromatographic condition and the average values were used. The standard deviation was always less than 2% with 0.5% as the usual precision. Retention factors were calculated from the retention times of the protein and solvent disturbance peaks. For each protein, the retention factors were determined at a minimum of four different ionic strengths at each eluent pH. Isocratic experiments were performed at pH 7.44, 8.85 and 9.22.

The performance of the chromatographic system was checked before every set of isocratic experiments with a linear gradient and a test mixture containing three proteins: nuclease A (wild type), mutant K116A and mutant K116E. A linear gradient from 50 mM sodium borate at pH 8.80 to 0.25 mM sodium chloride in 50 mM sodium borate at pH 8.8

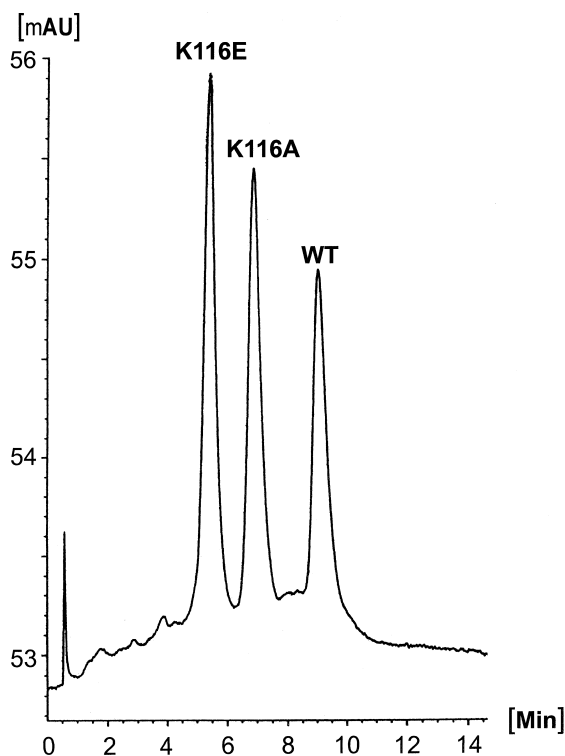


Fig. 1. Chromatogram of *S. nuclease A* (wt) and the mutants Lys116Ala (K116A) and Lys116Glu (K116E). Column POROS<sup>®</sup> HS; sulfopropyl, 10  $\mu$ m, 4.6 $\times$ 50 mm; eluent A, 50 mM sodium borate, pH 8.8; eluent B, 0.5 M NaCl in 50 mM sodium borate, pH 8.8. Linear gradient 0 min 100% A, 15 min to 50% B at 1 ml/min; detection at 280 nm; sample 25  $\mu$ l of 1 mg/ml protein dissolved in water.

in 15 min at a flow-rate of 1 ml/min was used; a typical chromatogram is shown in Fig. 1. The performance of the chromatographic system was considered satisfactory when the standard deviation of the three capacity factors was not larger than 1.0% RSD.

#### 4. Results and discussion

In this work the retention properties of *S. nuclease A* and 10 different mutants is investigated in cation-exchange chromatography. The wild type is a globular protein that contains 149 amino acids (MW

16 811 Da) and its iso-electric point is at pH 10.3. Its three-dimensional structure, except for the disordered amino acids in the vicinity of the N- and C-terminals, has been obtained from NMR measurements and X-ray crystallographic studies [22–24] at high resolution (1.7 Å). The mutants investigated here are stable molecules with nuclease A activity [25–27] which indicates that their tertiary structure is similar to that of nuclease A. This has also been confirmed in crystallographic studies of K116A, K116G, K116E, K116D, P117G and P117T [24,26–30].

##### 4.1. Net charge and charge distribution of *S. nuclease A* and mutants

The chromatographic experiments were performed at pH 7.44, 8.85 and 9.22. In order to interpret the chromatographic retention data, it is appropriate to investigate both the net charge and the charge distribution of the mutants at these pH values. In this work the mutants are divided into three classes based on net charge. The first class,  $q_1$ , consists of the wild-type *S. nuclease A* and its mutants in which the mutation is charge invariant in the experimental pH range (P47A, H124L, N118A, P117T, P117G). All proteins in the first class are therefore assumed to have the same net charge as the native *S. nuclease A* at any given eluent pH value. The second class ( $q_1 - 1$ ) consists of proteins where one basic amino acid in *S. nuclease A* has been substituted with a neutral amino acid (K116G and K116A) or where one neutral amino acid has been substituted by an acidic amino acid (N118D). Thus, at all pH values studied, the proteins in this class have one charge less than *S. nuclease A*. In the third class, ( $q_1 - 2$ ), the basic amino acid lysine at position 116 in *S. nuclease A* has been substituted by an acidic amino acid, glutamic or aspartic acid. The ( $q_1 - 2$ ) class of proteins consists of the mutants K116E and K116D and is assumed to have two charges less than *S. nuclease A* in the whole pH range examined.

Results of potentiometric titration experiments [21] have shown that the net charge of *S. nuclease A* is 10.4, 8.3 and 7.3 at pH 7.44, 8.85 and 9.22, respectively. Table 1 lists the mutants used in this work and the dependence of the net charge on the pH of the eluent is illustrated in Fig. 2. From the

Table 1  
Subclasses of *S. nuclease A* mutants according to their net charge compared to that of the wild type

Sub-class	Mutant code	Position of mutation	Residue replaced	
			In the Wild type	By residue to yield mutant
$q_1$	P47A	47	Proline	Alanine
	H124L	124	Histidine	Leucine
	N118A	118	Asparagine	Alanine
	P117T	117	Proline	Tyrosine
	P117G	117	Proline	Glycine
$q_1 - 1$	K116G	116	Lysine	Glycine
	K116A	116	Lysine	Alanine
	N118D	118	Asparagine	Glutamic acid
$q_1 - 2$	K116E	116	Lysine	Aspartic acid
	K116D	116	Lysine	Glutamic acid

electrophoretic properties of the mutants it has been concluded that, in these cases, the mutation does not induce any large changes in the size of the protein [20]. Therefore, change in surface area is negligible when the protein net charge is changed by single point mutations of the amino acid residue lysine 116. On the other hand, the dependence of the electrophoretic mobility of *S. nuclease A* on the pH of the eluent strongly suggests that this protein swells when the pH increases from 8.9 to 9.5. It is estimated that the corresponding increase in protein radius is 5.9 Å [20]. Some of our experiments were carried out at

pH 9.22, which lies between the above two values. Therefore, we assume that, upon raising the pH to this value, swelling causes the protein radius to increase by 3.0 Å.

In *S. nuclease A* the number and type of amino acid residues with protolytic properties are: five arginine, 23 lysine, four histidine, seven tyrosine, 12 glutamic acid and eight aspartic acid. In the experimental pH range 7.44–9.22, the protein net charge will change due to protonisation of the basic amino acid lysine and the phenolic amino acid tyrosine. The distribution of the lysine and tyrosine

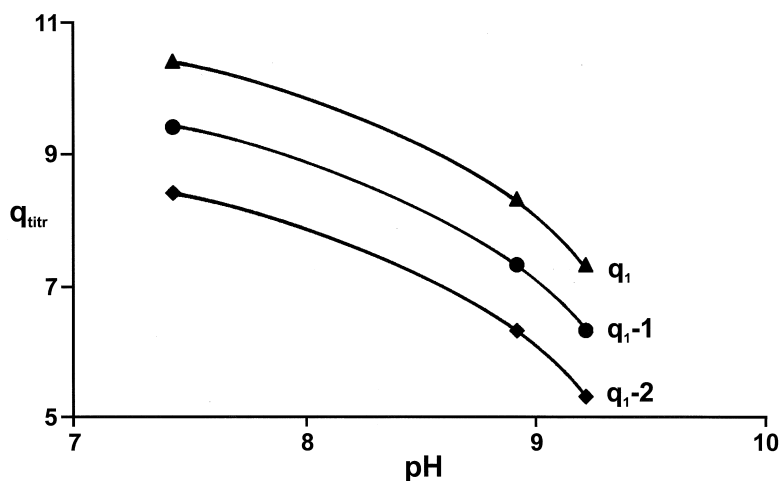


Fig. 2. Net charge of the proteins for the mutant subclasses, (◆)  $q_1$ , (●)  $q_1 - 1$ , and (▲)  $q_1 - 2$ , as a function of eluent pH. The values are based on experimental titration values of the wild type [20].

residues over the protein surface will therefore mainly determine the charge distribution. Fig. 3a and b show the crystallographic structure of *S. nuclease A* from two opposite angles. The first five and the last eight amino acids are omitted since these tails are disordered.

The numbers of lysine and tyrosine groups on the two sides shown in Fig. 3 are distinctly different. The side shown in Fig. 3a has 17 lysine and five tyrosine in comparison to the 13 lysine and four tyrosine on the side shown in Fig. 3b. Some of these residues are located at the border between the two sides and are therefore visible from both sides. As a result some of the lysine and tyrosine residues are counted twice and it is reasonable to assume that this excess of lysine and tyrosine groups is equally shared between the two protein surfaces shown in Figs. 3a and b, respectively. One additional lysine residue is located in the disordered terminal containing residues 1–5 (not shown); this group can also be assumed to be equally shared between the two sides of the protein. After correction for the shared groups, the algebraic sum of lysine and tyrosine residues assigned to the two sides shown in Fig. 3a and b becomes 17.5 and 12.5, respectively. Fig. 3a shows that 12 of these lysine and tyrosine residues are confined by the marked square with the borders positioned at Arg35, Lys110, Lys63/64 and Lys16/24. In conclusion, the uneven distribution of lysine and tyrosine residues results in an uneven charge distribution on the *S. nuclease A* surface in the investigated pH interval.

Since the mutants belonging to class  $q_1$  have the same net charge as *S. nuclease A*, it can be assumed that they also have the same charge distribution. The proteins belonging to class  $q_1 - 1$  are mutants of *S. nuclease A* with the point of mutation in position 116 or 118. It can be seen in Fig. 3a that these two positions are located on the highly charged side of the protein, but outside the square that represents the most densely charged part of the surface. Therefore, these mutants will also have an uneven charge distribution between the two sides of the protein surface. The same argument will be true for the two mutants belonging to class  $q_1 - 2$ , since in both cases the point of mutation is in position 116.

In sum, the tertiary structure of *S. nuclease A* shows that, when the pH of the surrounding solution

is between 7.44 and 10.3, the protein carries a positive net charge which is unevenly distributed over the protein surface. Furthermore, the mutants in classes  $q_1 - 1$  and  $q_1 - 2$  will have the same unevenness in charge distribution as the wild type.

#### 4.2. Ion-exchange chromatography

Isocratic ion-exchange chromatographic experiments were performed with eluents of different ionic strengths at pH 8.85 with the mutants shown in Table 1. In addition, one mutant from each subclass, P47A ( $q_1$ ), K116A ( $q_1 - 1$ ) and K116E ( $q_1 - 2$ ), was chromatographed isocratically at pH 7.44 and 9.22, respectively. The logarithm of the experimentally obtained retention factors was plotted versus the reciprocal square root of the ionic strength. It is recalled that the slab model, Eq. (6), predicts a linear dependence of  $\ln k'$  on  $1/\sqrt{I}$ . The results of all the chromatographic experiments are summarised in Table 2. The table shows the experimental values of the slope,  $S$ , of the  $\ln k'$  vs.  $1/\sqrt{I}$  plots, the linear regression correlation factors,  $r^2$ , and the estimated chromatographic charge,  $q_{\text{chr}}$ , calculated from Eq. (7). In obtaining these results the previously mentioned swelling was partly taken into account, which explains the 3.0 Å difference in protein radii between 20.9 Å and 23.9 Å at pH 8.85 and pH 9.22, respectively. It is assumed that the swelling is independent of the ionic strength of the eluent. The error in the chromatographic charge is estimated by using an error in the protein radius of  $\pm 1.7$  Å obtained from crystallographic studies of the protein [22–24]. Table 2 also presents the surface titration constants,  $K_p$ , as well as the titrimetric net charges,  $q_{\text{titr}}$ , of the mutants, both evaluated from the titration curve of the wild type [21].

The linear regression coefficients presented in Table 2 confirm the theoretically predicted linearity of the  $\ln k'$  vs.  $1/\sqrt{I}$  plot [17]. The slab model predicts that the slope of such plots should be equal for proteins having the same surface area and surface charge density. Since the size and charge of the proteins within each class used in this study are similar, they allow us to test this prediction. It is found that the values of  $S$  for the six different mutants of class  $q_1$  at pH 8.85 are all in the range

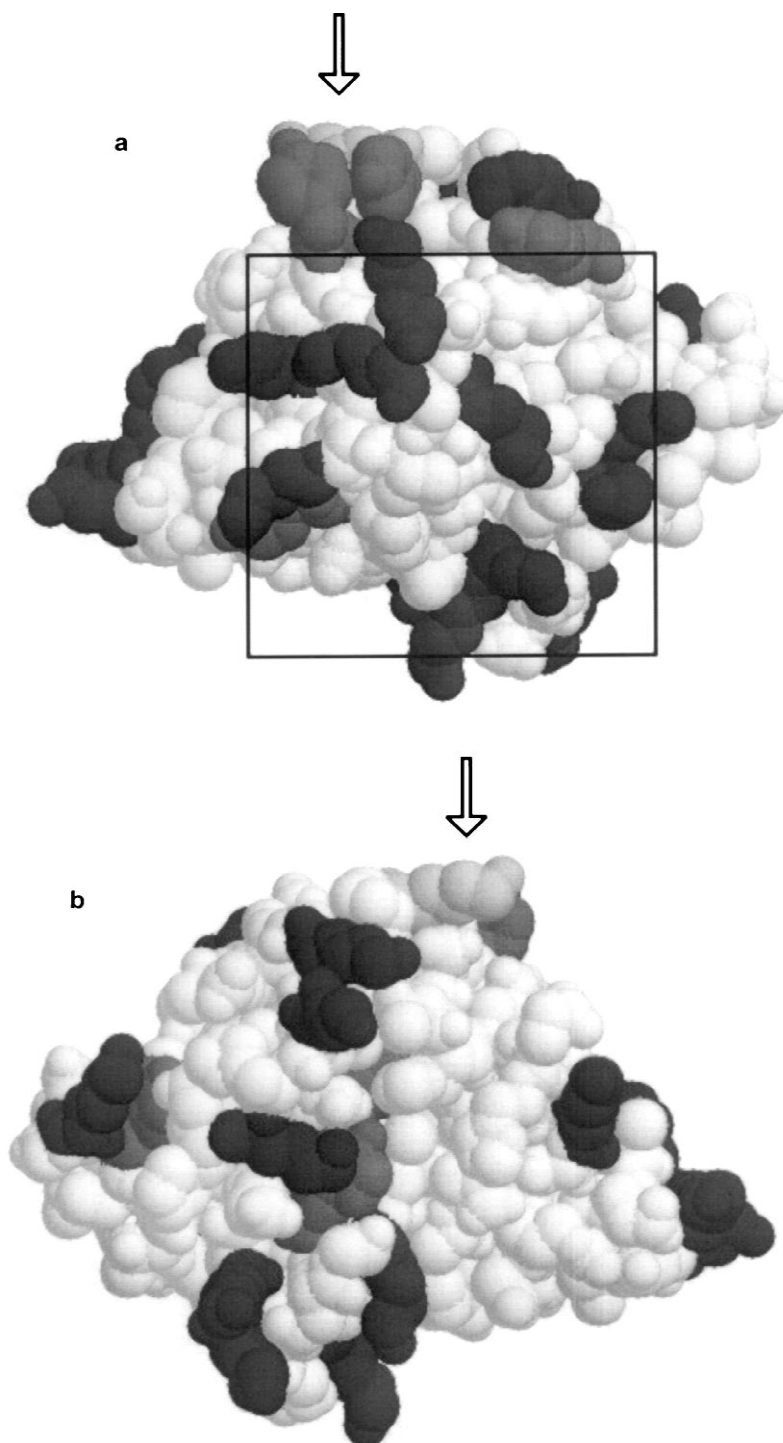


Fig. 3. Rasmol representation of the Brookhaven protein data base coordinates of *S. nuclease A* [22]. The first five and the last nine residues are not visible in this representation. The labelled residues are: Lys116 (light grey), indicated by an arrow, tyrosines (intermediate) and lysines (dark grey). The marked region in (a) contains about 12 of the 17.5 tyrosine and lysine residues situated on the more highly charged side of the protein at pH 7.44. (a) The highly charged site; (b) the side with low charge density.



Table 2

Slopes,  $S$ , of the  $\ln k'$  versus  $1/\sqrt{I}$  plots,  $\pm$  standard deviation their linear regression coefficient,  $r^2$ , and corresponding chromatographic charge,  $q_{\text{chr}}$ , vide (Eq. (7))  $\pm$  standard deviation, net charge,  $q_{\text{titr}}$ , based on the titration of S. nuclease A, at three different pH of the eluent. The range in the ratio between  $q_{\text{chr}}$  and  $q_{\text{titr}}$  is estimated from an error in  $q_{\text{titr}}$  of  $\pm 0.3$

Eluent pH	Mutant	Slope, $S$ (mol/dm <sup>3</sup> )	$r^2$	$K_p$	$q_{\text{titr}}^*$	$q_{\text{chr}}$	$q_{\text{chr}}/q_{\text{titr}}$
pH 7.44	P47A	8.72 $\pm$ 0.31	0.996	0.11	10.4	17.8 $\pm$ 0.4	1.6–1.8
	K116A	6.87 $\pm$ 0.22	0.998	0.12	9.4	15.7 $\pm$ 0.3	1.6–1.8
	K116E	6.28 $\pm$ 0.64	0.984	0.13	8.4	14.9 $\pm$ 0.8	1.6–1.9
pH 8.85	S.NucA	5.94 $\pm$ 0.46	0.989	0.35	8.3	12.5 $\pm$ 0.5	1.4–1.6
	P47A	5.15 $\pm$ 0.39	0.998	0.35	8.3	11.7 $\pm$ 0.5	1.3–1.5
	H124L	5.35 $\pm$ 0.28	0.994	0.35	8.3	11.9 $\pm$ 0.4	1.3–1.5
	N118A	5.63 $\pm$ 0.24	0.996	0.35	8.3	12.2 $\pm$ 0.3	1.4–1.6
	P117T	5.54 $\pm$ 0.23	0.997	0.35	8.3	12.1 $\pm$ 0.3	1.4–1.6
	P117G	5.13 $\pm$ 0.24	0.995	0.35	8.3	11.6 $\pm$ 0.3	1.3–1.5
	K116G	4.44 $\pm$ 0.21	0.995	0.38	7.3	10.6 $\pm$ 0.3	1.4–1.6
	K116A	4.18 $\pm$ 0.20	0.994	0.38	7.3	10.3 $\pm$ 0.3	1.3–1.5
	N118D	4.34 $\pm$ 0.15	0.997	0.38	7.3	10.5 $\pm$ 0.2	1.3–1.5
	K116E	3.54 $\pm$ 0.18	0.994	0.41	6.3	9.2 $\pm$ 0.3	1.4–1.6
	K116D	3.44 $\pm$ 0.24	0.991	0.41	6.3	9.1 $\pm$ 0.4	1.3–1.6
pH 9.22	P47A	3.44 $\pm$ 0.13	0.996	0.37	7.3	10.7 $\pm$ 0.2	1.4–1.6
	K116E	3.13 $\pm$ 0.18	0.990	0.42	6.3	9.8 $\pm$ 0.3	1.4–1.7
	K116A	2.18 $\pm$ 0.13	0.991	0.49	5.3	7.7 $\pm$ 0.3	1.3–1.6

from 5.13 to 5.95. Proteins in class  $q_1-1$  have slopes in the range 4.19–4.44 and for proteins in class  $q_1-2$  the slopes are in the range from 3.47 to 3.54. Statistical  $f$ - and  $t$ -tests show that, for a 95% confidence interval, the mutants within each class have slopes that are statistically indistinguishable from the other mutants within the same class. On the other hand, the same statistical test shows that the slopes for any two mutants from different classes are significantly different. Thus, for the data obtained at pH 8.85 the theoretical prediction that the slopes of the  $\ln k'$  vs.  $1/\sqrt{I}$  plots of the mutants with the same net charge are very similar is experimentally confirmed. However, as can be seen by examining the slope errors obtained at pH 7.44 and 9.22, two mutants at each pH have similar slopes and are not significantly different. The lack of significance in the  $S$  values for K116A and K116E at pH 7.44 is due to the large standard deviation in the  $S$  value for K116E resulting from fluctuations in the experimental retention times. At pH 9.22, P47A and K116A exhibit similar  $S$  values, which might be due to a decreased difference in net charge between the mutants due to deprotonation of Lys 116.

According to the slab model (Eq. (7)), the chro-

matographic charge,  $q_{\text{chr}}$ , of a protein is closely related to the value of the slope of the  $\ln k'$  vs.  $1/\sqrt{I}$  plot. Since the value for  $q_{\text{chr}}$  normally agrees well with the protein net charge obtained from titrimetric analysis [21], it is of interest to analyse how the  $q_{\text{chr}}/q_{\text{titr}}$  ratio varies with type of protein and pH of the eluent. The error in the  $S$  values results in an error in the calculated charge ratio, the latter error is influenced by possible errors in the net charge determined from titration. In the determination of the charge ratio, it is therefore assumed that the titrimetric charge has a mean error of  $\pm 0.3$ . Thereafter, an interval for the charge ratio is determined by dividing the highest chromatographic charge with the lowest titrimetric charge and vice versa. The obtained intervals for the charge ratio for all the mutants under investigation are also compiled in Table 2. It can be seen that the ratio varies between 1.3 and 1.7 for all mutants eluted at pH 9.22 and 8.85 and between 1.6 and 1.9 for the mutants eluted at pH 7.44. Ratios between 1.3 and 1.7 are somewhat higher than expected for a uniform charge distribution and agree well with the previously discussed uneven distribution according to the tertiary structure of the protein. The charge ratios estimated from the

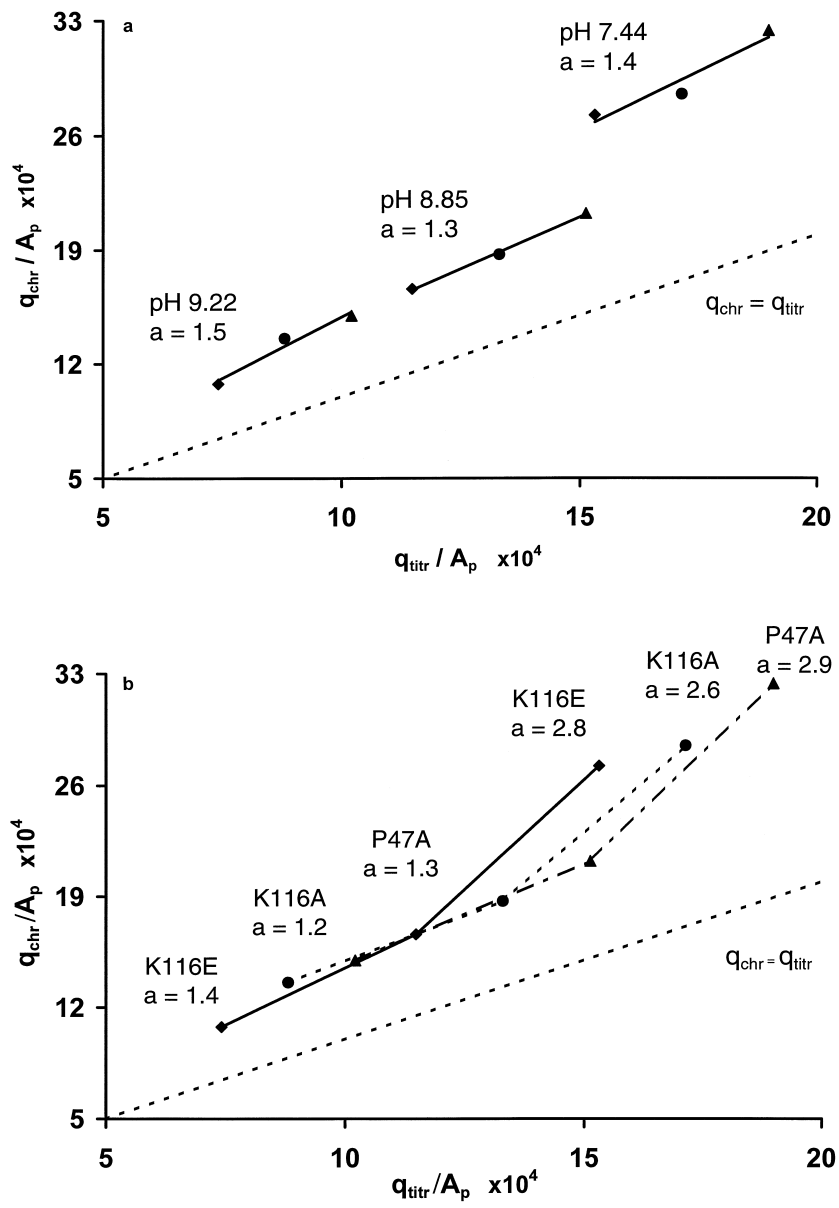


Fig. 4. Plots of the experimental chromatographic charge divided by the protein surface area versus the titrimetric charge divided by the protein surface area for the mutants (▲) P47A ( $q_1$ ), (●) K116A ( $q_1 - 1$ ) and (◆) K116E ( $q_1 - 2$ ) at the respective eluent pH of 7.44, 8.85 and 9.22. The dotted line represents identical chromatographic and titrimetric net charge, and the unit on both axes is the number of elementary charges per  $\text{\AA}^2$ . In (a), each line connects the data points for the three different mutants keeping the eluent pH value constant. In (b), each line connects the data points for a given mutant at the three different eluent pH values. Note that the experimental points in (a) and (b) are the same, the only difference being that the connecting lines are drawn differently. The lines in (b) are dash-dot, dotted and solid for P47A, K116A and K116E, respectively.

data indicate that the non-uniformity of the charge density becomes further pronounced when the pH is lowered to 7.44.

In the previous paragraph, the chromatographic implications of the charge distribution on the surface of different mutants were briefly examined. A closer analysis of the salt dependence of retention for the set of mutants gives further information about the effect of the pH of the eluent on the interaction between the mutants and the chromatographic surface. A change in the protein net charge due to mutation at a given point gives a different change in the charge distribution than a change in net charge due to an altered eluent pH. Since the primary charge parameter in the slab model is the charge density at the protein surface, and since the swelling changes the surface area, the ensuing analysis will address the change in  $q/A_p$ . Fig. 4a and b show plots of  $q_{\text{chr}}/A_p$  versus  $q_{\text{titr}}/A_p$  for the three mutants, representing the three classes. Both parts of the figure contain the same data points, but the connecting lines are drawn differently. A reference line representing  $q_{\text{chr}}/A_p = q_{\text{titr}}/A_p$  is also depicted. In Fig. 4a, data points obtained with different mutants at a given eluent pH are connected by a straight line. The slope of the lines represents the change in  $q_{\text{chr}}/A_p$  when  $q_{\text{titr}}/A_p$  changes by one unit due to mutation. The slopes of the three lines in Fig. 4a are 1.4 at pH 7.44, 1.3 at pH 8.85 and 1.5 at pH 9.22. These values are of the same order as the  $q_{\text{chr}}/q_{\text{titr}}$  values and indicate that the amino acids at the point of mutation contribute to the interaction. The fact that all lines have similar slope indicates that the contribution of the point mutation to the interaction is nearly the same for all mutants. It also shows that the contribution is the same over the pH range examined.

In Fig. 4b the lines connect the data points obtained for a given mutant at the three different eluent pH values. The slope of the lines represents the change in  $q_{\text{chr}}/A_p$  when  $q_{\text{titr}}/A_p$  changes with the eluent pH. In this case all three mutants exhibit the same pattern: the slope is around 1.3 when the net charge increases due to a change in pH from 9.22 to 8.85 and increases to around 2.8 when the pH is changed from 8.85 to 7.44. This indicates that the extra charge that the proteins gain between pH 8.85 and 9.22 is distributed somewhat unevenly between the two sides. This is in contrast to the case when the

pH changes from 8.85 to 7.44, where the increase in slope indicates that the two extra charges are placed mainly on one side of the protein, probably within the square marked in Fig. 3a.

## 5. Conclusions

In this work, the slab model is used to analyse the ionic strength dependence of retention for a set of mutants of *S. nuclease A* in cation-exchange chromatography. The experimental data confirm the theoretical expectation that the retention of mutants of the same size, net charge and charge distribution has the same ionic strength dependence. Thus, for proteins in ion-exchange chromatography, retention changes caused by changing the salt concentration in the eluent depend mainly on the protein charge or the charge distribution on its surface. A closer analysis of the chromatographic data also indicates that *S. nuclease A* and its mutants have an uneven surface charge distribution in the pH interval 7.4–9.2. Furthermore, the data also indicate that when the eluent pH decreases from 8.9 to 7.4, the two charges added to the *S. nuclease A* surface are mainly placed on one side of the protein. These interpretations of the experimental data are supported by an inspection of the molecular structure of *S. nuclease A*. The experimental data can also be used to shed light on the role of the amino acid in position 116 for the interaction between the protein and the ion-exchanger surface. An analysis of the data shows that position 116 makes only a moderately strong contribution to the interaction and that this contribution is independent of eluent pH.

## Acknowledgements

The chromatographic column employed in this study was generously donated by Istvan Mazsaroff of the Genetics Institute (Boston, MA, USA). The authors thank R.O. Fox and A. Hodel for preparation and characterisation of the *S. nuclease A* and its mutants, and for all the helpful discussions. Franka Kálmán held a Feodor-Lynen Fellowship from the Alexander von Humboldt Foundation. This work was

supported by grant GM No. 20993 from the NIH to Cs. Horváth.

## References

- [1] C.J.O.R. Morris, P. Morris (Eds.), *Separation Methods in Biochemistry*, 2nd Edition, Wiley, New York, 1976, p. 86.
- [2] N.K. Boardman, S.M. Partridge, *Biochem. J.* 59 (1955) 543.
- [3] A. Velayudhan, Cs. Horváth, *J. Chromatogr.* 367 (1986) 160.
- [4] W.R. Melander, Z.J. El Rassi, Cs. Horváth, *J. Chromatogr.* 469 (1989) 3.
- [5] I. Mazsaroff, L. Varady, G.A. Mouchawar, F.E. Regnier, *J. Chromatogr.* 499 (1990) 63.
- [6] V. Noinville, C. Vidal-Madjar, B. Sebille, *J. Phys. Chem.* 99 (1995) 1516.
- [7] J.N. Israelachvili, *Intermolecular and Surface Forces*, Academic Press, London, 1985.
- [8] G.J. Gouy, *J. Phys.* (1910) 457.
- [9] D.L. Chapman, *Am. Phys. J.* (1917) 475.
- [10] C.M. Roth, A.M. Lenhoff, *Langmuir* 9 (1995) 962.
- [11] C.M. Roth, A.M. Lenhoff, *Langmuir* 11 (1995) 3500.
- [12] C.M. Roth, K.K. Unger, A.M. Lenhoff, *J. Chromatogr. A* 726 (1996) 45.
- [13] J. Ståhlberg, B. Jönsson, Cs. Horváth, *Anal. Chem.* 63 (1991) 1867.
- [14] C.-H. Cai, V.A. Romano, P.L. Dubin, *J. Chromatogr. A* 693 (1995) 251.
- [15] W. Kopaciewicz, M.A. Rounds, J. Fausnaugh, F.E. Regnier, *J. Chromatogr.* 266 (1983) 3.
- [16] J. Ståhlberg, B. Jönsson, Cs. Horváth, *Anal. Chem.* 64 (1992) 3118.
- [17] J. Ståhlberg, B. Jönsson, *Anal. Chem.* 68 (1996) 1536.
- [18] D.J. Roush, D.S. Gill, R.C. Wilson, *J. Chromatogr. A* 653 (1993) 207.
- [19] M.L. Zoller, M. Smith, *Methods Enzymol.* 100 (1983).
- [20] F. Kálmán, S. Ma, R.O. Fox, Cs. Horváth, *J. Chromatogr. A* 705 (1995) 135.
- [21] F. Kálmán, S. Ma, A. Hodel, R.O. Fox, Cs. Horváth, *Electrophoresis* 16 (1995) 59.
- [22] T.R. Hynes, R.O. Fox, *Proteins Struct. Funct. Genet.* 10 (1991) 92.
- [23] R.O. Fox, P.A. Evans, C.M. Dobson, *Nature* 320 (1986) 192.
- [24] P.A. Evans, R.A. Kautz, R.O. Fox, C.M. Dobson, *Biochemistry* 28 (1989) 362.
- [25] T.R. Hynes, A. Hodel, R.O. Fox, *Biochemistry* 33 (1994) 5021.
- [26] P.A. Evans, C.M. Dobson, R.A. Kautz, G. Hatfull, R.O. Fox, *Nature* 329 (1987) 266.
- [27] A. Hodel, R.A. Kautz, R.O. Fox, *Protein Sci.* 4 (1995) 484.
- [28] A. Hodel, R.A. Kautz, M.D. Jacobs, R.O. Fox, *Protein Sci.* 2 (1993) 838.
- [29] A. Hodel, R.A. Kautz, M.A. Goodman, J.F. Gill, R.O. Fox, *Nature* 339 (1989) 73.
- [30] A. Hodel, R.A. Kautz, D.M. Adelman, R.O. Fox, *Protein Sci.* 3 (1994) 549.